High Power Laser Science and Engineering, (2024), Vol. 12, e58, 5 pages.
doi:10.1017/hpl.2024.35

HIGH POWER LASER SCIENCE AND ENGINEERING

LETTER

Sub-100 fs pulse generation from dispersion-managed mode-locked Er:ZBLAN fiber laser at 2.8 μm

Xiabing Zhou, Zhipeng Qin, and Guoqiang Xie

School of Physics and Astronomy, Key Laboratory for Laser Plasmas (Ministry of Education), Collaborative Innovation Center of IFSA (CICIFSA), Shanghai Jiao Tong University, Shanghai, China

(Received 22 February 2024; revised 18 April 2024; accepted 3 June 2024)

Abstract

We demonstrate the sub-100 fs pulse generation from a dispersion-managed mode-locked Er:ZBLAN fiber laser at 2.8 μm. Both numerical simulation and experiment demonstrate that stretched-pulse and dissipative soliton mode lockings coexist in the near-zero-dispersion region of a fluoride fiber laser. With fine dispersion management, the shortest pulse of 95 fs was obtained from the stretched-pulse mode-locked Er:ZBLAN fiber laser, with an average power of 280 mW and repetition rate of 52 MHz. To the best of our knowledge, this is the shortest pulse to date directly generated from a mid-infrared mode-locked fluoride fiber laser.

Keywords: dispersion management; femtosecond laser; mid-infrared; mode-locked laser

1. Introduction

Mid-infrared (MIR) pulse lasers have garnered widespread attention in recent years due to their potential applications in molecule spectroscopy, polymer processing, gas detection, precision laser surgery, etc.[1–6]. In particular, the MIR femtosecond laser, with an ultrashort pulse duration, is highly demanded as a fundamental source to extend the wavelength to long-wave infrared region via nonlinear frequency down-conversion or supercontinuum generation[7–9], and as a broadband seed pulse for chirped-pulse amplification[10].

The mode-locked fluoride fiber laser, featuring excellent beam quality, high efficiency and a simple structure, has become one of main ways to generate MIR pulse lasers. Saturable absorbers (SAs), such as the semiconductor saturable absorber mirror (SESAM) and low-dimensional materials, have been used for passive mode locking in the MIR region[11–16]. However, it is noteworthy that mode-locked fluoride fiber lasers enabled by real SAs generally have tens of picoseconds duration. The shortest picosecond pulse, obtained from a MIR fluoride fiber laser, was 4.7 ps in duration using frequency shift feedback based on an acousto-optic modulator[17]. The first MIR femtosecond fiber laser was realized based on the nonlinear polarization rotation (NPR) technique[18], delivering a pulse duration of 207 fs at 2.8 μm. By red-shifting the laser wavelength away from the vapor absorption lines, a pulse of 180 fs was produced from an NPR mode-locked Ho-doped fluoride fiber laser at 2.9 μm[19]. Since the fluoride fiber possesses anomalous dispersion in the MIR region, mode-locked lasers generally operate in the conventional soliton regime with a limited output energy and pulse duration[20–22]. Reducing the gain fiber length has been demonstrated to be effective in shortening the soliton duration. In this way, Gu *et al.*[23] achieved a remarkably short soliton of 131 fs. To date, plenty of investigations have indicated that conventional soliton mode locking is close to the duration limit. To obtain a shorter mode-locked pulse, one must change the mode-locking mechanism from the soliton regime to the stretched-pulse or dissipative soliton regime via intracavity dispersion management. However, due to the lack of suitable dispersion-compensation fiber in the MIR region, few dispersion-managed mode-locked fluoride fiber lasers have been investigated[24,25], and the reported results must rely on a discrete dispersive element such as a diffraction grating or bulk dispersive material. Huang *et al.*[24] employed a folded Martinez-type grating stretcher to compensate the dispersion of ZBLAN (ZrF_4-BaF_2-LaF_3-AlF_3-NaF) fiber and obtained the pulse of 126 fs at 2.8 μm.

Correspondence to: Z. Qin and G. Xie, School of Physics and Astronomy, Key Laboratory for Laser Plasmas (Ministry of Education), Collaborative Innovation Center of IFSA (CICIFSA), Shanghai Jiao Tong University, Shanghai 200240, China. Emails: lorance1205@sjtu.edu.cn (Z. Qin); and xiegq@sjtu.edu.cn (G. Xie)

In this paper, we fully investigated the pulse evolution of a dispersion-managed mode-locked fluoride fiber laser when the net cavity dispersion changed from negative to positive. Both stretched-pulse and dissipative soliton mode-lockings were obtained depending on the net cavity dispersion. In the near-zero-dispersion region, we numerically and experimentally demonstrated the coexistence of the dissipative soliton and stretched pulse at the same net cavity dispersion. With fine dispersion management by germanium (Ge) rods, we demonstrated the generation of a sub-100 fs pulse from a mode-locked Er:ZBLAN fiber laser in the near-zero-dispersion region. To the best of our knowledge, this represents the shortest pulse directly generated from MIR mode-locked fluoride fiber lasers to date.

2. Numerical simulation

Based on nonlinear Schrödinger equation[26], we first simulated the dispersion-managed NPR mode-locked Er:ZBLAN fiber laser. The numerical model considered the impact of vapor absorption on the mode-locked spectrum. Initiating from a random noise, the steady state of pulse evolution was achieved after numerous roundtrips. The net cavity dispersion varies from –0.3 to +0.2 ps^2, and the variation of output pulse duration is presented in Figure 1, marked with three dispersion regions: the net negative dispersion (I-pink), the near-zero dispersion (II-yellow) and the net positive dispersion (III-blue). In region (I), the stretched pulse had a femtosecond duration, gradually shortening as the net cavity dispersion increased. As the net cavity dispersion went into region (II), both the stretched pulse and dissipative soliton were produced at the same net cavity dispersion,

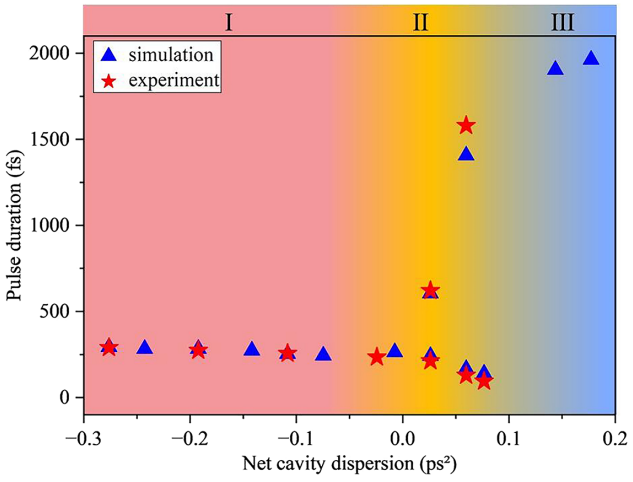

Figure 1. Evolution of pulse duration versus the net cavity dispersion. Numerical simulation is conducted with the following key parameters: fiber length of 3.07 m, fiber dispersion β_{fiber} of –0.09 ps^2/m, fiber nonlinear coefficient γ_{fiber} of 1.72×10^{-4} (W·m)$^{-1}$ and Ge dispersion β_{Ge} of +1.68 ps^2/m[16,20–23]. The experimental data are obtained based on the experimental setup depicted in Figure 4.

depending on the intracavity pulse energy. The duration of the higher-energy stretched pulse continued to narrow, while the lower-energy dissipative soliton was widened rapidly with the increase of net cavity dispersion. When the net cavity dispersion was increased further into region (III), only a picosecond dissipative soliton could be obtained.

Figure 2 presents a detailed evolution of the pulse duration and spectrum along the cavity in the near-zero-dispersion region (II). Two distinct states are obtained at the net cavity dispersion of +0.06 ps^2 with different output energies. The intracavity pulse reaches the shortest duration after passing through the NPR part in both states. Subsequently, the large normal dispersion, introduced by the Ge rod, broadens the pulse, and the pulse is gradually recompressed within the Er:ZBLAN gain fiber (Figures 2(a) and 2(b)). Different from the dissipative soliton, the stretched pulse experiences a larger pulse breathing ratio of 67, allowing one to extract the energy more efficiently. The pulse spectrum is broadened by the self-phase modulation (SPM) effect in the rear part of fiber (Figure 2(c)) and the pulse duration remains stable for a short distance due to the balance of dispersion and nonlinearity. The dissipative soliton exhibits notably different spectral evolution as the pulse propagates within the fiber, as shown in Figure 2(d). There is no significant change in the spectral profile during the propagation, indicating that the SPM effect is relatively weak and the dominant influence on pulse duration is the dispersion effect. Numerically, the femtosecond stretched pulse tends to form at the higher pump power level, while the dissipative soliton dominates at the lower pump power level.

Due to the influence of vapor absorption lines on the spectrum, many dips are observed from the mode-locked spectra obtained from the output coupler (OC), as shown in Figures 2(c) and 2(d). The modeled stretched pulse with the broad spectrum had a corresponding pulse duration of 166 fs, as shown in Figure 3(a), and its chirp characteristic ($d\phi/dt$) was checked in the pulse duration, with a nonlinear chirp. The modeled dissipative soliton exhibits a significant linear positive chirp in the pulse duration of 1.41 ps (Figure 3(b)), which can be dechirped to 0.84 ps.

3. Experiment and results

Guided by the numerical simulation, we established the NPR mode-locked Er:ZBLAN fiber laser, as depicted in Figure 4, and experimentally investigated its operation by varying the net cavity dispersion. The experimental parameters were consistent with those used in the simulation. An Er:ZBLAN fiber, with 3.07 m length, 7% (mole fraction) Er doping, a core diameter of 15 μm and a cladding diameter of 250 μm, was pumped by a 976 nm laser diode. The two aspheric lenses L_1 and L_2 (f = 12.7 mm) were used to couple the pump beam into the fiber and collimate the output laser beam. The two ends of the fiber were 8-deg angle-cleaved to

https://doi.org/10.1017/hpl.2024.35 Published online by Cambridge University Press

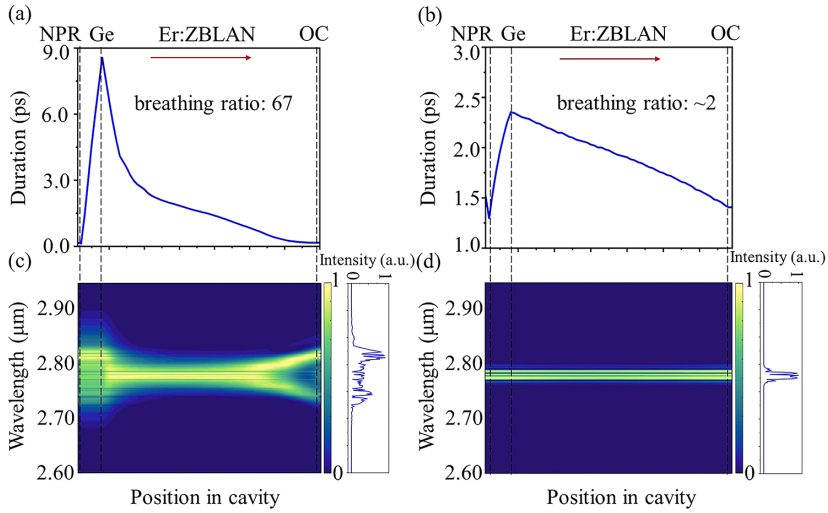

Figure 2. Simulation results of dispersion-managed mode-locked pulses at the net cavity dispersion of +0.06 ps^2. Evolution of pulse duration: (a) the stretched pulse and (b) the dissipative soliton. Evolution of the spectral profile and output spectrum: (c) the stretched pulse and (d) the dissipative soliton.

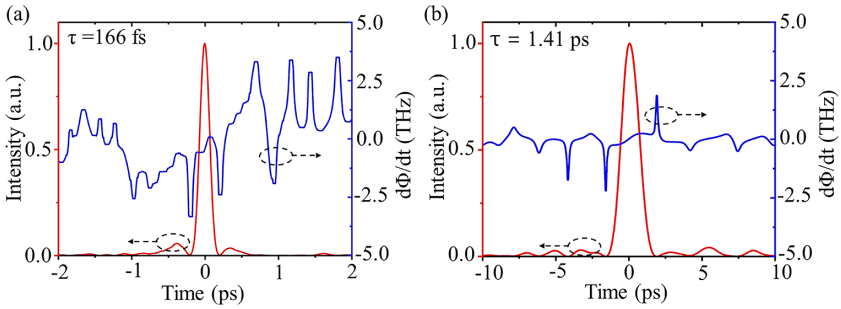

Figure 3. Output pulse profiles and chirps of (a) the modeled stretched pulse and (b) the modeled dissipative soliton at the net cavity dispersion of +0.06 ps^2.

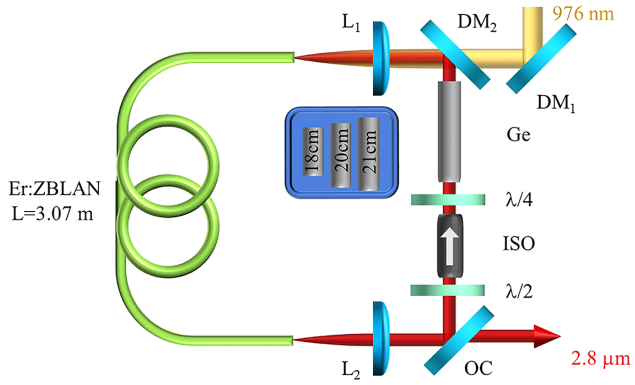

Figure 4. Schematic of a dispersion-managed mode-locked Er:ZBLAN fiber laser. λ/4, quarter-wave plate; λ/2, half-wave plate; ISO, polarization-dependent isolator; $DM_{1,2}$, dichroic mirrors; $L_{1,2}$, aspheric lenses.

suppress parasitic oscillation. An OC with 40% transmission was placed after the gain fiber. Mode-locking operation was achieved using NPR components, which included a half-wave plate, an isolator and a quarter-wave plate. To reduce the mode-locking threshold, we controlled intracavity pulse propagation along the direction of the pump light. Ge rods of varying lengths were employed for dispersion management with negligible insertion loss and nonlinear effect. Its large dispersion ($\beta_{Ge} \approx -19 \times \beta_{fiber}$ @ 2.8 μm) originates from the substantial change of refractive index near the band gap.

Without the dispersion compensation by the Ge rod, the mode-locked Er:ZBLAN fiber laser operated in the conventional soliton regime, delivering an output pulse duration of 290 fs (Figure 1) and an energy of 1.1 nJ. As we increased the length of the Ge rod in the cavity, the mode-locked laser gradually transited from a conventional soliton to stretched-pulse mode locking, with the trend of pulse shortening. When the length of the Ge rod was 20 cm, corresponding to the net cavity dispersion of +0.06 ps^2, two distinct mode-locked states were observed experimentally (Figure 5). At a high pump power of 4.20 W, stretched-pulse mode locking was achieved with an output pulse energy of 5.4 nJ. The pulse duration was 130 fs, assuming a sech^2 pulse profile (Figure 5(a)). Additional positive or negative dispersion compensation outside the cavity no longer led to a shorter duration of pulse compression. Thus, a nearly transform-limited femtosecond pulse was experimentally obtained. When the launched pump power was reduced to 3.30 W, the

https://doi.org/10.1017/hpl.2024.35 Published online by Cambridge University Press

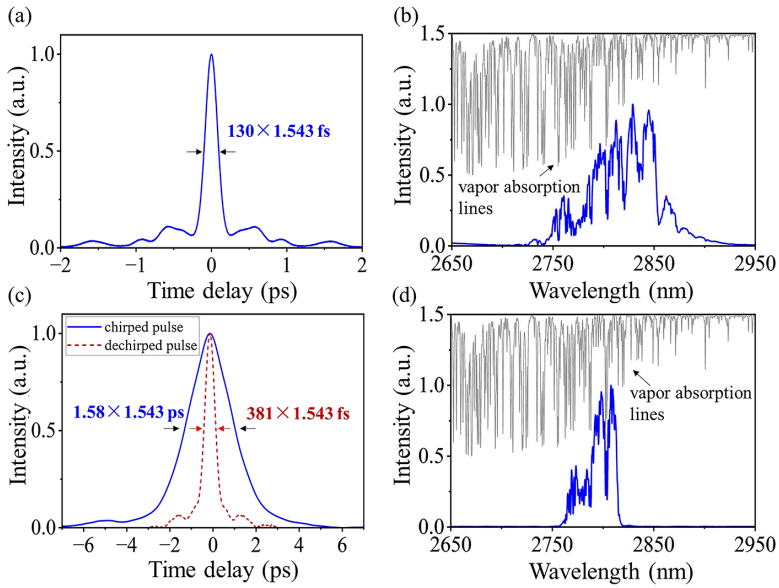

Figure 5. Experimental results of dispersion-managed mode-locked Er:ZBLAN fiber laser at the net cavity dispersion of +0.06 ps^2. (a) Autocorrelation trace and (b) spectrum of the stretched pulse. (c) Autocorrelation trace and (d) spectrum of the dissipative soliton.

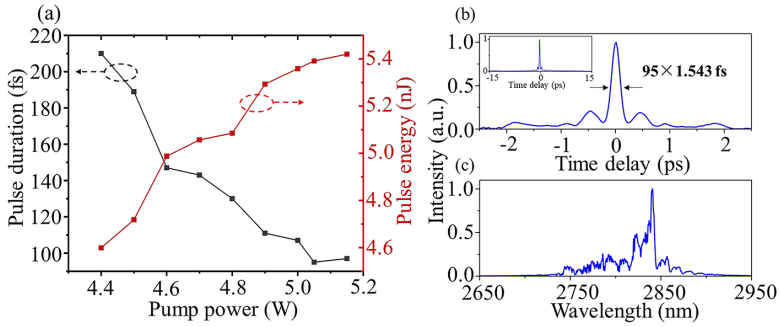

Figure 6. Experimental results of stretched-pulse mode-locked Er:ZBLAN fiber laser at the net cavity dispersion of +0.08 ps^2. (a) Dependence of pulse duration and energy on the pump power, (b) autocorrelation trace (inset: autocorrelation trace within the 30 ps window), and (c) optical spectrum.

mode-locked fluoride fiber laser switched from a stretched pulse to a dissipative soliton, with a lower output energy of 3.5 nJ. Actually, the dissipative soliton could also be obtained just by rotating the wave plates because the cavity nonlinear loss was closely related to the orientations of the wave plates. In the dissipative soliton regime, the output pulse exhibited significant positive chirp, with a pulse duration of 1.58 ps (Figure 5(c)). After dechirping with two pairs of Ge prisms, the pulse was compressed to 381 fs. The optical spectrum of the pulses exhibited the characteristic steep spectral edges of a dissipative soliton (Figure 5(d)). Although no physical bandpass filter was inserted into the cavity, there was an artificial birefringence filter in the NPR mode-locked fiber lasers. Due to the bandpass limitation of this artificial filter, the effective gain of the laser has a narrow bandwidth[27]. Many dips in the spectra were the consequence of vapor absorption lines (Figures 5(b) and 5(d)).

With a focus on pulse shortening, we further increased the Ge rod length to 21 cm, resulting in the net cavity dispersion of +0.08 ps^2. As the pump power increased, the stretched-pulse energy increased while the pulse duration continuously decreased, as depicted in Figure 6(a). At the pump power of 5.05 W, we obtained pulses with duration as short as 95 fs and pulse energy of 5.4 nJ, as illustrated in Figure 6(b). No pulse splitting was observed in a broader window of 30 ps (inset of Figure 6(b)). Fine dispersion management makes intracavity pulses evolve with a larger breathing ratio, effectively reducing nonlinear phase accumulation and facilitating the generation of higher pulse energy. Then, assisted by the combined effects of nonlinear spectral broadening and negative dispersion compression, ultrashort pulses can be easily obtained. The optical spectrum is shown in Figure 6(c) with a central wavelength of approximately 2.8 μm. The shortwave component was absorbed much more by the vapor due to the free-space propagation in the cavity. Continuing to increase the pump power beyond 5.05 W did not result in further shortening in pulse duration, but rather posed an increased risk of damaging the facet of the fiber. When the net cavity dispersion exceeds +0.08 ps^2, it is difficult to obtain the picosecond

https://doi.org/10.1017/hpl.2024.35 Published online by Cambridge University Press

mode-locking operation experimentally because the NPR-based mode-locking threshold exceeds the damage threshold of the fluoride fiber facet.

4. Conclusion

In conclusion, we numerically and experimentally demonstrated a dispersion-managed mode-locked Er:ZBLAN fiber laser at 2.8 μm. When the net cavity dispersion changed from –0.3 to +0.2 ps^2, both the stretched-pulse and dissipative soliton mode-lockings were realized in the MIR region. We also demonstrated the coexistence of the stretched-pulse and dissipative soliton mode-locking in the near-zero-dispersion region. With fine dispersion management by the Ge rod, stretched pulses as short as 95 fs were directly generated from the Er:ZBLAN fiber laser at 2.8 μm with a pulse energy of 5.4 nJ at the net cavity dispersion of +0.08 ps^2. To the best of our knowledge, this is the first sub-100 fs pulse directly generated from MIR mode-locked fluoride fiber lasers. Such femtosecond mode-locked fiber laser sources are very attractive in applications such as MIR supercontinuum generation, chirped-pulse amplification and ultrafast dynamics studies.

Acknowledgements

This work was supported by the National Key Research and Development Program of China (No. 2023YFB3507404), the National Natural Science Foundation of China (Nos. 62005161, 62075126 and 62325506), the Innovation Program of Shanghai Municipal Education Commission (No. 2023ZKZD19) and the Fundamental Research Funds for the Central Universities.

References

1. G. Ycas, F. R. Giorgetta, E. Baumann, I. Coddington, D. Herman, S. A. Diddams, and N. R. Newbury, Nat. Photonics **12**, 202 (2018).
2. M. Yan, P. Luo, K. Iwakuni, G. Millot, T. W. Hänsch, and N. Picque, Light Sci. Appl. **6**, 76 (2017).
3. K. Hashimoto, T. Nakamura, T. Kageyama, V. R. Badarla, H. Shimada, R. Horisaki, and T. Ideguchi, Light Sci. Appl. **12**, 48 (2023).
4. A. H. Nejadmalayeri, P. R. Herman, J. Burghoff, M. Will, S. Nolte, and A. Tünnermann, Opt. Lett. **30**, 964 (2005).
5. S. Amini-Nik, D. Kraemer, M. L. Cowan, K. Gunaratne, P. Nadesan, B. A. Alman, and R. J. D. Miller, PLoS ONE **5**, e13053 (2010).
6. J. Ma, Z. P. Qin, G. Q. Xie, L. J. Qian, and D. Y. Tang, Appl. Phys. Rev. **6**, 021317 (2019).
7. L.-R. Robichaud, S. Duval, L.-P. Pleau, V. Fortin, S. T. Bah, S. Châtigny, R. Vallée, and M. Bernier, Opt. Express **28**, 107 (2020).
8. Y. Cui, H. Huang, Y. Bai, W. Du, M. Chen, B. Zhou, I. Jovanovic, and A. Galvanauskas, Opt. Lett. **48**, 1890 (2023).
9. J. Swiderski, Prog. Quant. Electron. **38**, 189 (2014).
10. Y. C. Zhou, Z. P. Qin, X. B. Zhou, and G. Q. Xie, High Power Laser Sci. **10**, e41 (2022).
11. J. F. Li, D. D. Hudson, Y. Liu, and S. D. Jackson, Opt. Lett. **37**, 3747 (2012).
12. Z. Qin, X. Chai, G. Xie, Z. Xu, Y. Zhou, Q. Wu, J. Li, Z. Wang, Y. Weng, T. Hai, P. Yuan, J. Ma, J. Chen, and L. Qian, Opt. Lett. **47**, 890 (2022).
13. Z. Qin, G. Xie, C. Zhao, S. Wen, P. Yuan, and L. Qian, Opt. Lett. **41**, 56 (2016).
14. Z. Qin, G. Xie, J. Ma, P. Yuan, and L. Qian, Photonics Res. **6**, 1074 (2018).
15. C. H. Zhu, F. Q. Wang, Y. F. Meng, X. Yuan, F. X. Xiu, H. Y. Luo, Y. Z. Wang, J. F. Li, X. J. Lv, L. He, Y. B. Xu, J. F. Liu, C. Zhang, Y. Shi, R. Zhang, and S. N. Zhu, Nat. Commun. **8**, 14111 (2017).
16. J. C. Wei, P. Li, L. P. Yu, S. C. Ruan, K. Y. Li, P. G. Yan, J. C. Wang, J. Z. Wang, C. Y. Guo, W. J. Liu, P. Hua, and Q. T. Lü, Chin. Opt. Lett. **20**, 011404 (2022).
17. M. R. Majewski, R. I. Woodward, and S. D. Jackson, Opt. Lett. **44**, 1698 (2019).
18. S. Duval, M. Bernier, V. Fortin, J. Genest, M. Piché, and R. Vallée, Optica **2**, 623 (2015).
19. S. Antipov, D. D. Hudson, A. Fuerbach, and S. D. Jackson, Optica **3**, 1373 (2016).
20. Y. C. Wang, F. Jobin, S. Duval, V. Fortin, P. Laporta, M. Bernier, G. Galzerano, and R. Vallée, Opt. Lett. **44**, 395 (2019).
21. N. Bawden, O. Henderson-Sapir, S. D. Jackson, and D. J. Ottaway, Opt. Lett. **46**, 1636 (2021).
22. L. Yu, Z. Tang, J. Liang, Q. Zeng, J. Wang, X. Luo, J. Wang, P. Yan, F. Dong, X. Liu, Q. Lue, C. Guo, and S. Ruan, Opt. Lett. **48**, 1830 (2023).
23. H. A. Gu, Z. P. Qin, G. Q. Xie, T. Hai, P. Yuan, J. G. Ma, and L. J. Qian, Chin. Opt. Lett. **18**, 031402 (2020).
24. J. Huang, M. Pang, X. Jiang, F. Köttig, D. Schade, W. He, M. Butryn, and P. S. Russell, Optica **7**, 574 (2020).
25. Z. P. Qin, G. Q. Xie, H. A. Gu, T. Hai, P. Yuan, J. G. Ma, and L. J. Qian, Adv. Photonics **1**, 065001 (2019).
26. G. P. Agrawal, *Nonlinear Fiber Optics*, 5th ed. (Elsevier, 2013), p. 43.
27. L. M. Zhao, D. Y. Tang, X. A. Wu, and H. Zhang, Opt. Lett. **35**, 2756 (2010).

https://doi.org/10.1017/hpl.2024.35 Published online by Cambridge University Press